

5

Evaluation of recharge processes and the impacts of irrigation on groundwater by using CFCs and radiogenic isotopes in the Silao-Romita basin, Mexico

10

author's pre-version of the paper:

15

Horst A., Mahlkecht J., Broder J. Merkel, Ramon Aravena, Yann R. Ramos-Arroyo (in print) Use of environmental isotopes and gaseous tracers for estimating groundwater recharge and flow in the Silao-Romita Aquifer, Guanajuato, Central Mexico. Hydrogeology Journal, Springer-Verlag Heidelberg. ISSN: 1431-2174 (Paper) 1435-0157 (Online)

Axel Horst*, Jürgen Mahlkecht, Broder J. Merkel, Ramon Aravena, Yann R. Ramos-Arroyo

20

A. Horst* (axelhorst@itesm.mx), **J. Mahlkecht** (jurgen@itesm.mx)

Centro de Estudios del Agua

Tecnológico de Monterrey

Ave. Eugenio Garza Sada No. 2501,

CP 64849 Monterrey, N.L., México

25

Tel: 0052 81 81582261 Fax 0052 81 8358 2000 5563

B. J. Merkel (merkel@geo.tu-freiberg.de)

Department of Geology

Technische Universität Bergakademie Freiberg

30

Gustav Zeunerstrasse 12,

09596 Freiberg, Germany

R. Aravena

Department of Earth and Environmental Sciences

35

University of Waterloo

Waterloo, Ontario, Canada N2L 3G1

Y. R. Ramos-Arroyo

Facultad de Ingeniería en Geomática e Hidráulica

40

Universidad de Guanajuato

CP 36000 Guanajuato, GTO., México

* corresponding author

Abstract

45 The recharge processes in the overexploited aquifer of the Silao Romita basin, Central Mexico,
were investigated by means of gaseous tracers (CFCs) and radioactive isotopes (C-14, tritium). CFC
concentrations varied between 0.06 and 12 pmol/l (CFC-11), 0.03 and 1.7 pmol/l (CFC-12), and
<0.01 and 0.23 pmol/l (CFC-113). Chlorofluorocarbon concentrations are controlled by irrigation
return flow which became apparent by the comparison with tritium. Tritium activities ranged from 0
50 to 3.5 TU. The calculated mean residence times of 70 to more than 300 years are considerably
lower than the ages estimated based on the CFCs data. These data showed that CFCs were not
appropriate for groundwater dating in this particular area but the CFCs were suitable as a qualitative
measure of the magnitude of irrigation return flow which proved to be a significant source of
recharge in the irrigated areas. Radiocarbon activities were in the range of 6 to 109 pmC. Carbon-13
55 values varied between -11.9 and -7.2 ‰ VPDB. Modelling of carbon isotopes with NETPATH
along a plausible flowpath reveals considerable influences of exchange with soil CO₂ and carbonate
dissolution. Radiocarbon data indicate at least in one case the existence of groundwaters with
residence times of more than 10,000 years.

60

Key Words: recharge processes, chlorofluorocarbons, radioactive isotopes, irrigation
return flow, Central Mexico

65

Introduction

The Silao-Romita study area (1,950 km²) is located in the Lerma-Chapala river system in Central Mexico. Water supply in this region occurs principally by groundwater. Since the fifties of the last century the demand for water has increased due to growing population and expanding agriculture.

70 Groundwater resources from approximately 2,000 pumping wells are used mainly for farming (87%). Eleven percent are pumped for drinking water, and one percent for industry and stock-farming respectively. The extraction by pumping amounts to $408 \cdot 10^6$ m³/yr. The recharge rate is lower than the abstraction rate, thus the water table has decreased annually by 2-4m within the last 10 years because of a deficit of approximately $33 \cdot 10^6$ m³/yr (CEAG 2003).

75 Previous studies in Silao-Romita comprise geological and geophysical investigations in order to describe the subsurface geometry and chemistry of the aquifer system (CEASG 1999; SAPAL 2001). Due to long-term consequences of overexploitation, recent efforts have been undertaken to refine the conceptualization of the functioning of the Silao-Romita aquifer (CEAG 2003; COREMI et al. 2004).

80 Up to now, the recharge pattern and distribution of groundwater residence times of this strongly modified groundwater regime is hardly understood. The lack of this knowledge of these elements precludes effective management techniques for a sustainable groundwater use. Irrigation return flow is assumed but processes and distribution have not been specified or qualified yet.

Tritium and chlorofluorocarbons (CFCs) are normally used to detect recent recharge and to estimate
85 the residence time of younger groundwaters having recharged within the last 60 years (e.g. Beyerle et al. 1999; Happell et al. 2006;). Groundwaters of longer residence times can be traced by means of radiocarbon (¹⁴C). Numerous studies applied ¹⁴C to determine groundwater ages or to estimate paleorecharge (e.g. Weissmann et al. 2002; Zuber et al. 2004).

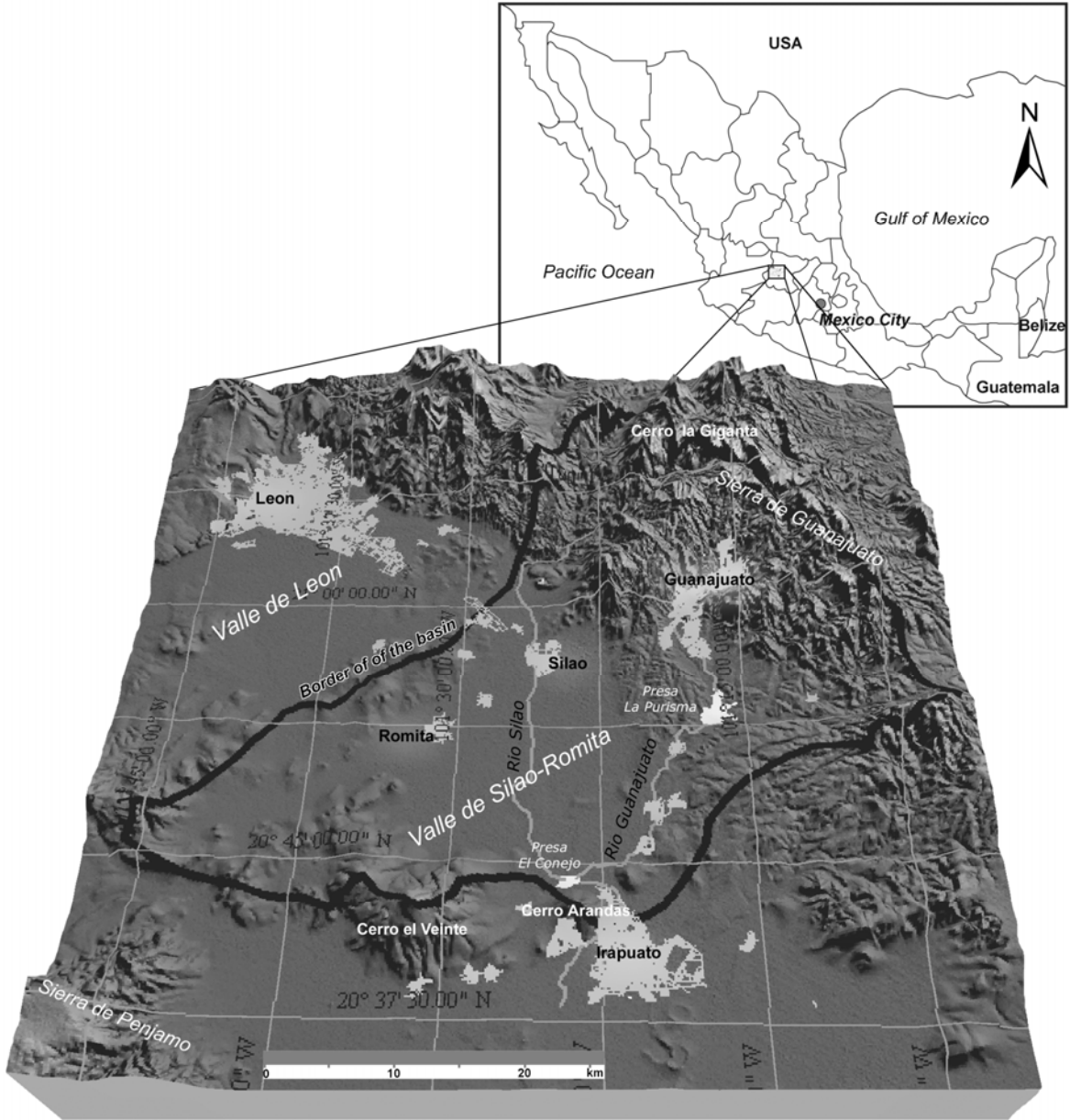
This study aims for providing a better understanding of the recharge processes and age distribution
90 in the aquifer of Silao-Romita by means of a combination of environmental tracer techniques. It
also intends to qualitatively evaluate the impact of return flow from irrigated areas.

1 Study Area

The Silao-Romita aquifer system is a sub-basin of the Guanajuato river catchment that is located in
the Guanajuato state between the northern latitudes 20°42' and 21°09' and the western longitudes
95 101°10' and 101°44' containing the urban areas of Guanajuato City, Silao, Romita and Irapuato
(Fig. 1). The maximum extension in SW – NE direction is approximately 67 km and in NW – SE
direction 48 km. It is limited in northeast by the Sierra de Guanajuato (Highland of Guanajuato), in
northwest by the Valle de León (Valley of León), in the south by the Sierra de Penjamo, Cerro el
Veinte and Cerro Arandas, and in the west by uprisings of volcanic origin.

100 The major elevations within the area reach altitudes of about 2,800 metres above sea level (masl)
and are principally situated in the Sierra de Guanajuato. The plains have altitudes of 1,740-1,780
masl in the valley of Silao-Romita.

The average annual precipitation amounts to 622 mm and the average annual actual
evapotranspiration to 516 mm (COREMI et al. 2004). Eighty percent of total rain occurs in summer
105 (July-September). Precipitation in the Sierra de Guanajuato reaches up to 800 mm. The annual
average air temperature is 18.5 °C, with a minimum of 15 °C in January and maximum of 23 °C in
May. The investigation area is drained primarily from north to south. The principal river, Rio
Guanajuato, has a mean discharge of 115 Mm³/yr (CEAG 2003).



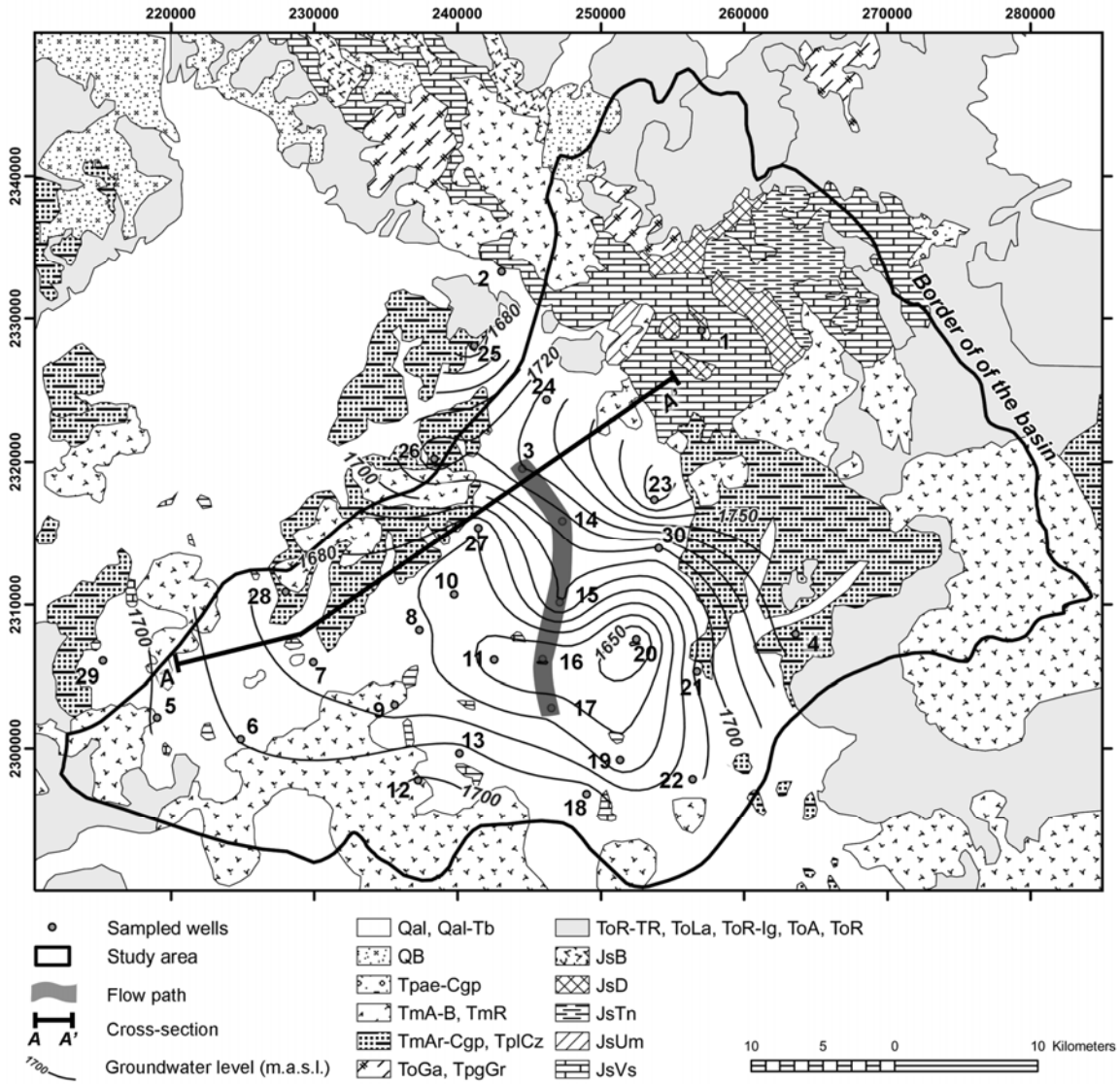
110 **Fig. 1** Digital elevation model of the study area based on SRTM3 data of the NASA (accessible through: <ftp://e0srp01u.ecs.nasa.gov/srtm/version2/SRTM3>). Illustrated elevations are 20-fold inflated.

2 Hydrogeological characteristics

115 The investigation area is part of two large physiographic units: The Cinturón Volcánico Transmexicano (Mexican Neovolcanic Belt) and the Mesa Central (Central Highland). The former covers the southern and larger part of the study area, the latter forms the Sierra de Guanajuato. The tectonic development of these physiographic units is amply described (e.g. Burbach et al. 1984; Pardo and Suarez 1993). The investigation area can be classified in two larger geological groups.

120 The first group is represented by the Sierra de Guanajuato in the north-eastern region of the investigation area. It corresponds to the older Mesozoic and Tertiary geologic units containing sedimentary, volcanoclastic and intrusive rocks, as well as minor quantities of consolidated conglomerates. The mountains coincide with faults having the same NW-SE – orientation like for example the Falla El Bajío (El Bajío Fault), but are also intersected by faults following the NE-SW-
125 orientation (Falla Aldana) representing the general orientation of the majority of the faults in the area (Aranda-Gomez et al. 1989; Nieto-Samaniego et al. 1996;).

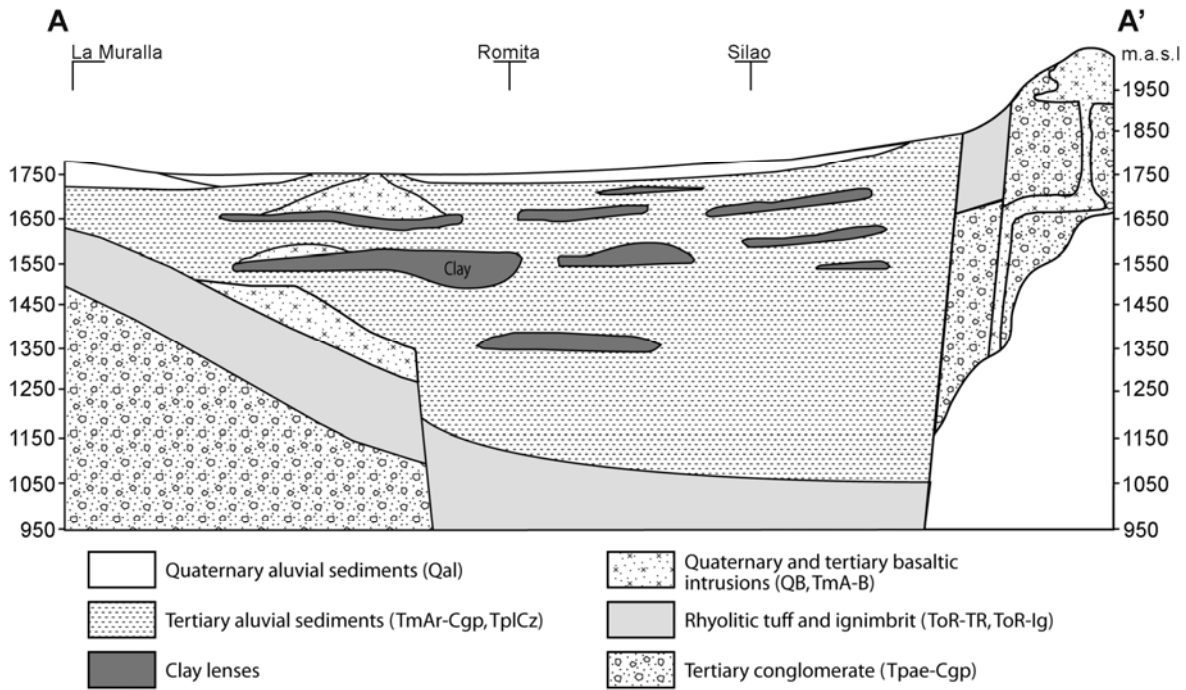
The second group is represented by the south-western part of the study area. It consists of juvenile formations of volcanic material of the middle Tertiary and Quaternary and alluvial deposits. The sediments forming the relatively plain valley of Silao-Romita are partially overlain by Quaternary
130 volcanic rocks (CEASG, 2001). These sediments contain the studied aquifer which might be connected to adjacent aquifers in the northwest (León) and eventually south (Irapuato). Fig. 2 presents the distribution of the stratigraphic units.



135 **Fig. 2** Geology (modified from COREMI et al. 2004), and sampling sites. Qal and Qal-Tb: recent
 140 sedimentary deposits; QB: quarternary basalt; TmArCgp and TplCz: tertiary sedimentary unit of the
 Miocene and Pliocene; Tmr and TmA-B: volcanic rocks of the Miocene; ToR-TR, ToLa, ToR-Ig, ToA
 and ToR: volcanic rocks of the Oligocene; TpaeCgp: Conglomerate of Guanajuato; ToGa and TpgGr:
 tertiary intrusions; JsUm: ultramafic unit San Juan de Otates; JsD: diorite Tuna Mansa; JsTn: tonalite
 Cerro Pelón; JsB: basalt La Luz; JsVs: volcano-sedimentary unit. 3-14-15-16-17: assumed flowpath for
 NETPATH modelling; A-A': cross-section illustrated in Fig. 3. Axes values in UTM coordinates.
 Groundwater levels, measured during the sampling campaign, are given in metres above sea level
 (masl).

The aquifer system of Silao-Romita consists of two zones: an unconfined aquifer close to the
 surface with a maximum thickness of 30 m. Underlying this aquifer is the so-called regional aquifer
 145 with widely differing extension and thickness. The border between these two aquifers is constituted

by numerous lenses of clay (COREMI et al. 2004). With a thickness of up to 1,000 m, the regional aquifer appears generally unconfined. Figure 3 shows a schematic cross section of the aquifer system modified from Foster et al. (2004).

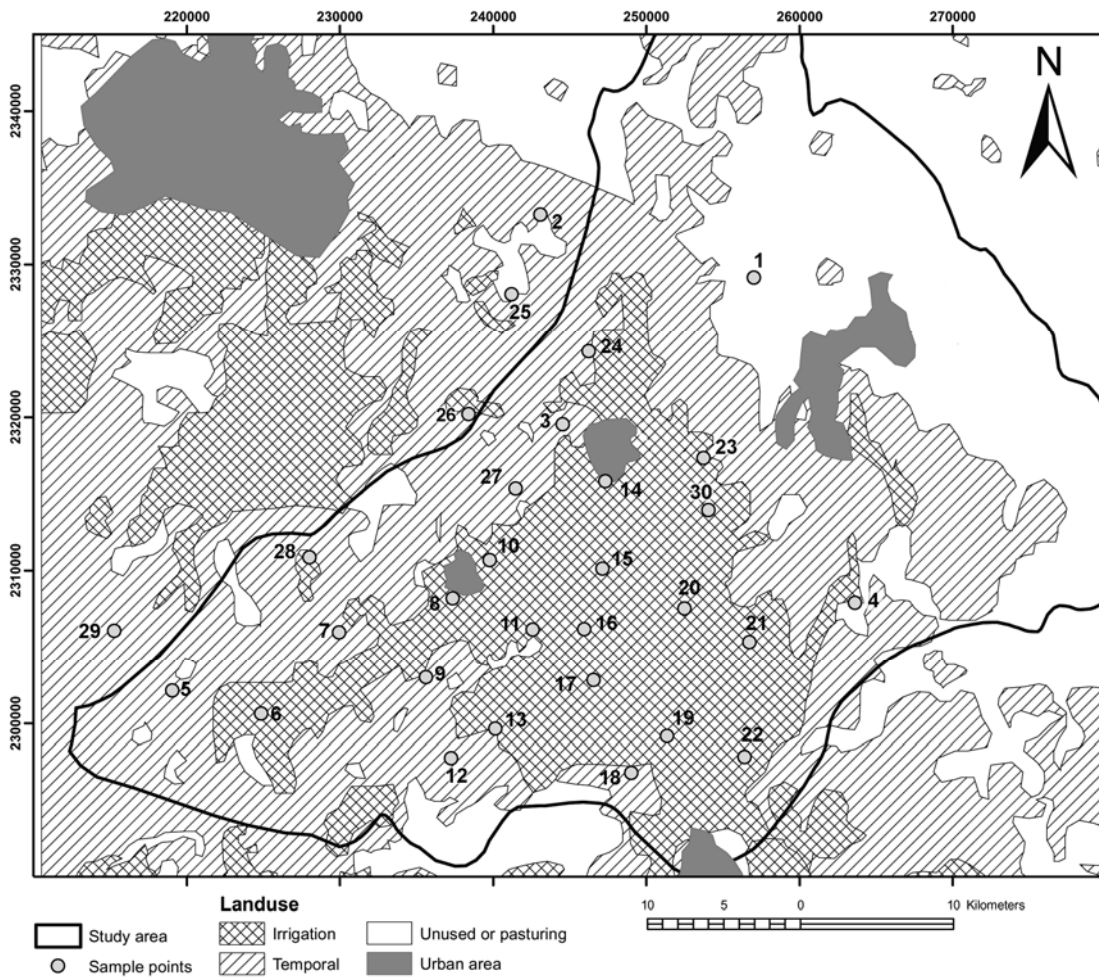


150 **Fig. 3 Schematic geological cross section of the Silao-Romita aquifer, modified from Foster et al. (2004), see also A-A' in Fig. 2.**

Original groundwater flow is supposed to pass the basin from north to south following the natural gradient of the terrain (CEASG 1998). Due to severe abstraction rates and drawdown, nowadays, water flows from the margins to the central part of the basin (see Fig. 2).

155 Groundwater recharge originates from various natural and artificial sources. Horst et al. (2007) described the origin of groundwater in the study area by means of stable isotopes (^{87}Sr , ^{13}C , ^2H and ^{18}O) indicating a ternary mix of (i) infiltrating waters, (ii) a laterally inflowing component of fissure waters and (iii) deep calcite-saturated groundwater. Deuterium and oxygen-18 data in some water showed the effect of evaporation. The isotope data are within a small range of 2 ‰ $\delta^{18}\text{O}$ which
 160 proves similar recharge conditions and/or well mixture of groundwaters.

Discharge occurs primarily through irrigation wells. Spring water volume is comparatively small and the number of springs has decreased during the last decades, which was also observed in adjacent basins (Mahlknecht et al. 2004; Navarro de León et al. 2005). The use of irrigation water is inefficient. CEAG (2003) found that 82% of the water production wells are operated ineffectively applying methods like ditch irrigation. Therefore large quantities of water are lost by evaporation or seepage. CEASG (1999) estimated the return flow to approximately 15 % of overall recharge. Figure 4 presents the landuse. It becomes apparent that the irrigation district covers approximately one third of the study area.



170 Fig. 4 Landuse in the investigation area.

3 Methodology

Thirty samples (28 pumping wells and 2 springs) were taken in October 2005, for chemical, isotopic and CFC analyses. The wells that were not in operation were purged at least for 15 minutes before sampling. The springs were sampled directly at the outflow. Anion and cation samples were filtered (0.45 μm MILLIPORE nitrocellulose filters) and stored cool in new pre-rinsed HDPE bottles. Cation samples were acidified with ultrapure HNO_3 ($\text{pH} < 2$) for preservation.

Field parameters (pH, conductivity, temperature) were measured directly at each well [WTW (Wissenschaftlich-Technische Werkstätten, Weilheim, Germany) Multi 350i; pH-Electrode SenTix41]. Calibration of the pH-probe was performed at every sampling point. Alkalinity was obtained by titration with 0.02 N H_2SO_4 to pH 4.3.

Analyses of major chemical elements were done by the Hydrochemical Laboratory of the Technische Universität Bergakademie Freiberg, Germany. The anions were analyzed with the (ion chromatographs) Eppendorf Biotronik IC2001, and cations with the Merck Hitachi Equipment (L-6200A pump, D-6000A interface and L-3720 conductivity detector). The standard deviations are 1.5 mg/l (Na^+), 0.53 mg/l (Ca^{2+}), 0.22 mg/l (Mg^{2+}), 0.77 mg/l (NO_3^-) and 0.81 mg/l and (SO_4^{2-}) respectively.

The analysis of tritium was performed at the Laboratory for Natural Radionuclides of the Technische Universität Bergakademie Freiberg, Germany. Tritium was analyzed through counting β -decay events in a liquid scintillation counter (“Quantulus”). The 300 ml samples were distilled and in cylindrical cells of the IAEA-type electrolytically enriched by the factor of 17 ± 0.5 . The detection limit of the method is 0.2 TU. Since regional Tritium precipitation data were not available an input function was compiled based on the two closest stations of the IAEA-GNIP (Global Network of Isotopes in Precipitation: Chihuahua (28.63°N and 106.07°W); Veracruz (19.2°N and 96.13°W)) by taking the mean of the annual mean input of these two stations. Because the

monitoring didn't start before 1962 and ended in 1988, input values before and after this interval had to be estimated. For input values before 1962 an exponential function was used assuming that the natural production before 1952 was 4 TU. Between 1962 and 1988 some gaps were interpolated linearly. After 1988 an annual decrease of the tritium activity of 5.5% (Clark and Fritz 1997) was assumed (Fig. 5).

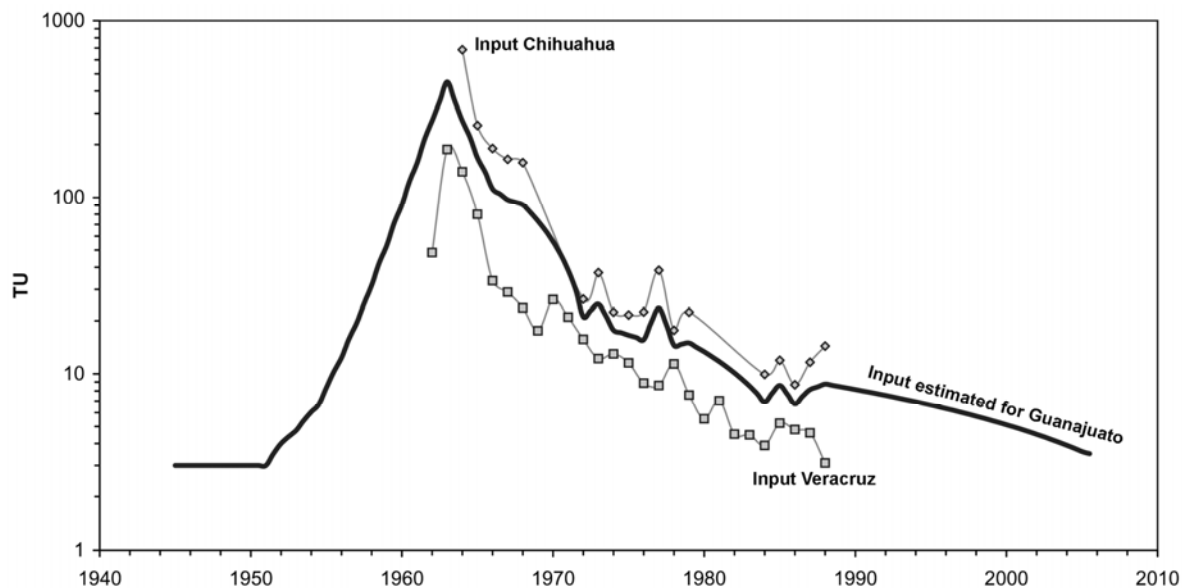


Fig. 5 Estimated input function of tritium using the GNIP-IAEA-network data of the two closest stations Veracruz and Chihuahua.

For analyses of CFCs special 500 ml glass bottles stored in water filled containers were used to prevent contamination. The Trace-Gas-Laboratory Dr. Oster, Wachenheim (Germany) performed the analysis using an electron capture detector and gas chromatography (GC-ECD). Details of preparation and analysis are described in Oster et al. (1996). The detection limit is 0.01 pmol/l for CFC-113. The input function is assumed to be valid for the whole northern hemisphere due to atmospheric mixing. Measurements in Colorado (USA) and Adrigole/Macehead (Ireland) show similar values (Engesgaard et al. 2004). The air mixing ratios were calculated using the equations of Weiss and Price (1980) and the constants of Warner and Weiss (1985) and Bu and Warner (1995). To account for the required recharge temperature in the calculation the mean annual air temperature

of the investigation area (18.5°C) and as recharge elevation 1,800 masl were assumed. Salinities were measured during the field campaign. A significant time lag is described by Cook and Solomon
215 (1995) for the transport of trace gases through thick unsaturated zones. CFC concentrations at the top of the water table are lower than the atmospheric CFC contents. The same authors found that thicknesses of less than 10 m cause a time lag of approximately 2 years which in most cases is negligible. The depth to the groundwater in the valley of Silao-Romita is mostly more than fifty meters. To account for the large unsaturated zone thickness correction models have to be applied.
220 Cook and Solomon (1995) developed an analytical solution assuming an exponential increase of CFC concentrations in the unsaturated zone.

Carbon-13 determination was performed by the Environmental Isotope Laboratory (EIL), University of Waterloo, Canada, by acidifying the samples with H₃PO₄ to pH 4 and purifying the CO₂ using cold distillation. Carbon dioxide was then transferred into mass spectrometric vessels and
225 analysed on the MM-903 spectrometer for $\delta^{13}\text{C}_{\text{DIC}}$ with respect to VPDB. For calibration the internal standard EIL30 was used. For radiocarbon (¹⁴C) analysis, a CO₂ aliquot was extracted by the EIL-laboratory (same method as for ¹³C) and sent in glass ampoules to the IsoTrace Laboratory at the University of Toronto, Canada. There, the CO₂ was converted into graphite by the reaction of carbon dioxide with molten lithium, which formed Li₂C₂ and then produced acetylene. Graphite
230 then was deposited epitaxially from the acetylene by a high voltage electrical discharge as 3-mm diameter discs (approximately 250 µg of carbon per disc) onto the two electrodes (targets). Every target contains one disc and is analysed separately with two ¹⁴C standards (NBS Ox1) in different runs. The analyses were carried out by Accelerator Mass Spectrometry (AMS). The ¹³C/¹²C ratio being analysed at the same time is used to correct the ¹⁴C/¹²C ratio for isotope fractionation during
235 analysis.

Since carbonate dissolution may take place in the aquifer, the modified Pearson $\delta^{13}\text{C}$ mixing model was applied for correction (Clark and Fritz 1997). Furthermore, for selected wells along a flowpath,

the influence of distinct carbon reservoirs was evaluated with the geochemical code NETPATH (v. 2.13, Plummer et al., 1994). For correction of ^{14}C activities exchange with soil- CO_2 and dilution with ^{14}C -free carbon from carbonate mineral reactions were considered. There is no evidence of sulphate reduction or methanogenesis in the aquifer and ^{14}C activities are not corrected for these processes. Incorporation of geogenic CO_2 is another possible process but in most wells it is unlikely because of its location in Tertiary and Quaternary alluvial sediments. Only sample 2, 7 and 28 might be influenced by these processes because of its chemical composition and/or the location of the wells close to faults. Clark and Fritz (1997 and references therein) mention $\delta^{13}\text{C}$ ratios of -6 ‰ for mantle derived CO_2 . Sample 2, 7 and 28 have $\delta^{13}\text{C}$ values of -9.3 ‰ or lower and is considered to be small in comparison to carbonate dissolution or soil- CO_2 . Modelled ^{14}C -residence times are only considered geologically meaningful if the calculated mineral mass transfer (i.e. dissolution vs. precipitation) and the $\delta^{13}\text{C}_{\text{TIC}}$ is in agreement with the calculated mineral saturation state of the groundwater and the measured $\delta^{13}\text{C}_{\text{TIC}}$, respectively (Matter et al. 2005). The measured $\delta^{13}\text{C}_{\text{carbonates}}$ concentrations on 3 samples of distinct sediment layers are -1.9, -5.2 and -6.6 ‰ respectively. Mahlknecht et al. (2004) reported a range of -2 to +2‰ in the adjacent basin.

4 Results

Results of field parameters, analysis of some anions and cations as well as isotope and trace gas contents of the samples are presented in detail in the Appendix. The results of field parameters reveal influences of waters of different origin. Likewise in former reports (COREMI et al., 2004; SAPAL, 2001), in the present study thermal water was detected. Well 29, well 30 and spring 2 have temperatures above 30°C. These wells are situated along or close to the Romita, El Bajío and Aldana faults and represent thermal water. Lower temperatures in the range of 23 to 25°C are found in the plain and irrigated areas. Conductivity normally ranges between 430 and 1,400 $\mu\text{S}/\text{cm}$. In two cases conductivities of 2,450 (well 28) and 2,740 $\mu\text{S}/\text{cm}$ (well 7) are more than twice as high as the

others due to the high sulphate, bicarbonate and sodium concentrations. The pH was between 7.2 and 7.8 at almost all sampling points, except for the thermal water of sample no. 2 (8.7).

In a former study (CEASG, 1999); one out of six wells had detectable tritium (1.3 TU). The current
265 study also documented relatively low values. Only seven out of thirty samples show tritium
activities larger than 1 TU. Almost half of the results present 2- σ ranges being larger than the
measured activities. The highest values were detected at the edge of the Sierra de Guanajuato
(sample no. 1). This sampling point with 3.5 TU is an exception, because it is a spring sitting
between impermeable consolidated diorite and fractured permeable andesite. It can be assumed that
270 the residence time is relatively short and the determined activity corresponds to the recent
atmospheric tritium content. The estimated local input function in Fig. 4 indeed shows the same
value for the year 2005.

CFC-11 concentrations vary between 0.06 and 12 pmol/l, CFC-12 between 0.03 and 1.7 pmol/l, and
CFC-113 between <0.01 and 0.23 pmol/l. The equivalent air concentration range from 5 to 1,065
275 pptv (parts per trillion by volume), from 10 to 559 pptv, and from 3 to 69 pptv, respectively.
Considering the corresponding input functions (Böhlke 2004) CFC-11 shows a significant deviation
from CFC-12 and also from CFC-113. CFC-12 and CFC-113 are more consistent (Fig. 6). In Fig. 6a
the samples plot generally below the exponential model (EM) curve. This lower CFC-11/CFC-12
ratio may be due to degradation of CFC-11 (Lindsey et al. 2003). It could also be possible that
280 CFC-12 is enriched but in Fig. 6b the tracer pairs of CFC-12 and CFC-113 plot within the regions
bounded by piston and exponential flow curves. It has been demonstrated that these two compounds
are less degraded in groundwaters than CFC-11 (e.g. Plummer and Busenberg, 2000). Fig 6b also
shows that the tracer pairs arrange along the exponential model line. The CFC-11 value of 1,065
pptv in well 24 indicates contamination because it is four times as high as the peak of atmospheric
285 input values in 1994. Furthermore well 11 and 14 appear to be CFC-12-contaminated since the
tracer pairs plot outside the curve-bounded region (Fig. 6b).

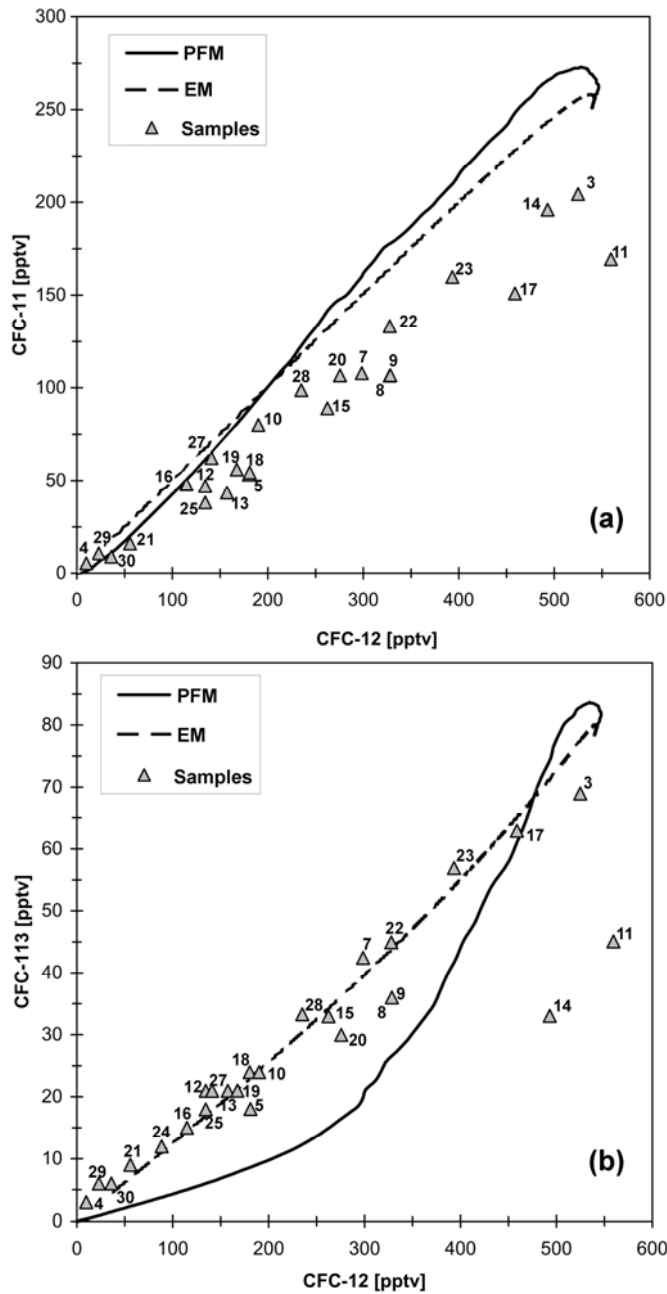


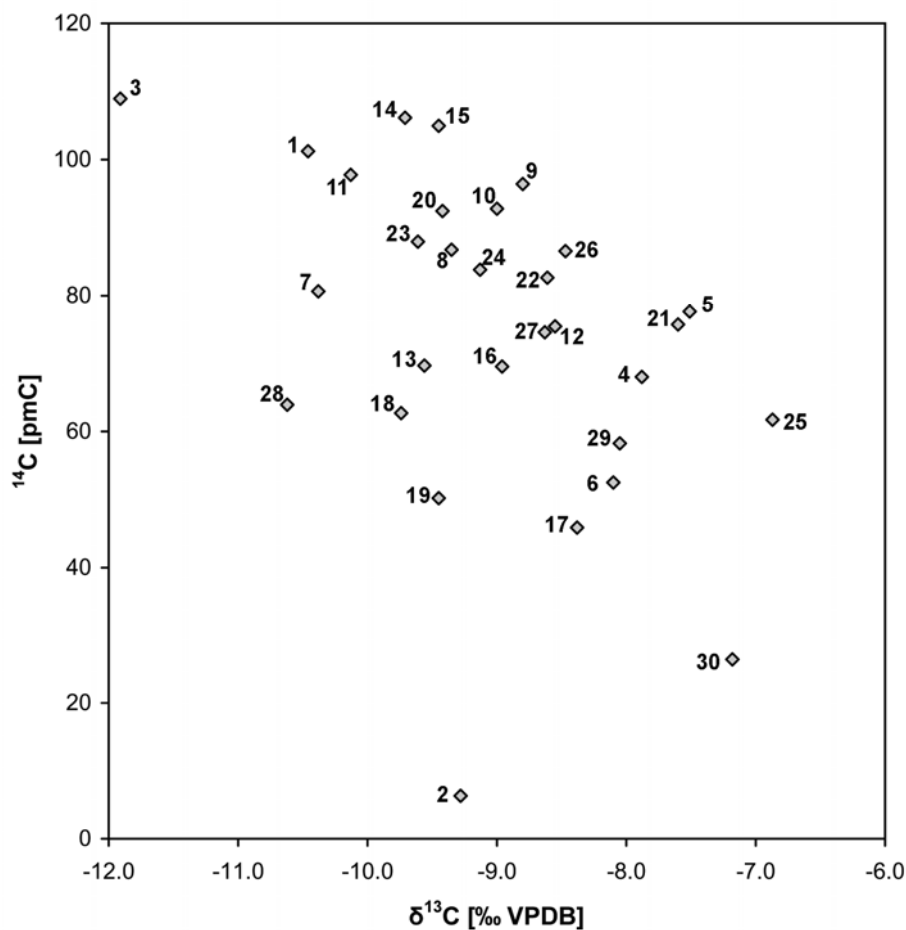
Fig.6 Tracer concentrations plotted for piston flow (PFM) and exponential flow (EM) and measured tracer pairs CFC-11 vs. CFC-12 (a) and CFC-113 vs. CFC-12 (b). Curves end at date of sample.

310

The thick unsaturated zone was considered applying the correction model of Cook and Solomon (1995). The obtained correction values are only applicable directly for the piston flow model. To correct the mean residence times resulting from EM calculations the time lag must be applied for every flow line. The difference between the corrected and uncorrected mean residence time is the mean time lag. It describes the influence of the unsaturated zone on the mean groundwater ages calculated with the exponential model. As a simplified constraint a constant water table depth in the catchment area of every well was considered applying the measured groundwater levels. The calculated time lags for CFC-12 are presented in Table 1.

The $\delta^{13}\text{C}$ values range between -7.2 and -11.9 ‰ VPDB, and the ^{14}C activities vary between 6 and 109 pmC. Fig. 7 shows an inverse correlation between ^{14}C and $\delta^{13}\text{C}$ values indicating that dissolution of carbonatic aquifer rock material has taken place during the groundwater flow which is reflected in the enrichment in ^{13}C and the depletion in ^{14}C contents. This correlation is confirmed by nonparametric tests (Spearman's rho and Kendall's tau b) which yield significance levels of 0.01 respectively.

The conventional calculation of uncorrected radiocarbon yields residence times of up to 23,000 years. Carbonate corrected residence times reach up to 14,000 years.



320

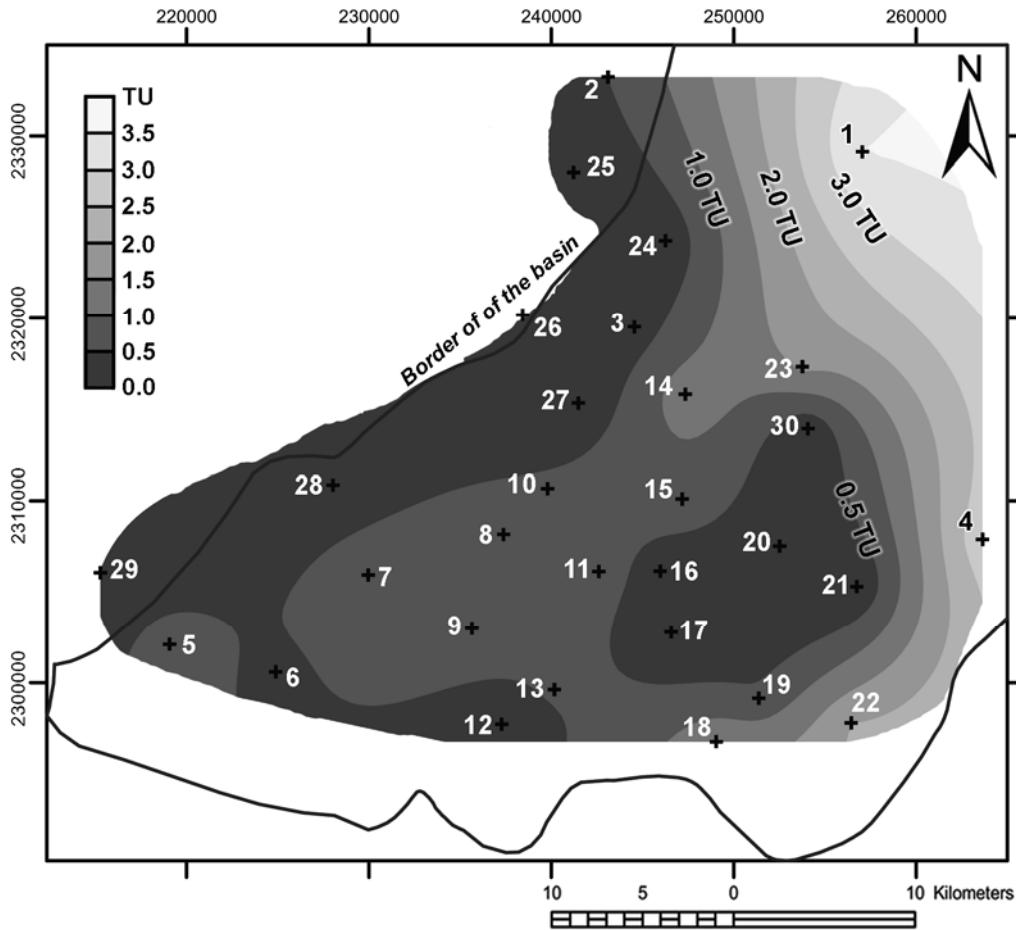
Fig. 7 Plot of ^{14}C activities versus $\delta^{13}\text{C}$ ratios.

5 Discussion

5.1 Residence time calculations

325 To determine the residence times (RTs) of groundwater the geometry of the aquifer has to be taken into account. The aquifer of the investigated basin is mostly unconfined and the wells penetrate the saturated zone to a depth of up to 300 m. They are almost always screened completely. These conditions match best with the exponential model (Zuber 1986). The validation with CFCs in Fig. 6b confirmed this assumption. The mean residence times (MRTs) for the exponential model are
330 within the range of 73 and >300 years, with exception of spring 1 which shows recent recharge (see Table 1). The low tritium activities can only be considered as a rough estimation since they are close to the detection limit. For example well 9 has a 2σ -range of ± 0.4 TU. Considering this analytical uncertainty the corresponding mean residence time could be between 200 and 500 years.

Figure 8 presents the distribution of tritium in the study area. Higher activities (light grey colours)
335 are found in the Sierra de Guanajuato and in the south-eastern region. The lower basin generally shows low tritium values (dark grey). The distribution indicates the natural recharge regions. Higher values demonstrate shorter residence times and consequently potentially greater recharge. This distribution may also indicate existence of recharge fronts migrating from the eastern elevations to the basin.



340

Fig. 8 Distribution of tritium activities. Values indicate activities in tritium units (TU)

CFCs are normally used to validate tritium MRTs especially when activities are low or results are ambiguous. The calculation of the MRTs reveals considerable differences between tritium and CFC-12 or CFC-113. If the calculated time lags are applied, the differences become even larger (see Table1). An explanation for this apparent incongruence is the intensive agriculture in the study area. When groundwater is abstracted for irrigation, its CFC concentration is increased by the higher CFC content in the air. The extracted groundwater, whose CFC concentration has now risen (rejuvenated), re-infiltrate through return flow processes and increases the concentration of CFC in groundwater. Tritium activities are not affected by return flow.

350 Most of the ^{14}C results are not appropriate for residence time calculation because of the mentioned effects of enrichment through return flow. Despite the uncertainties, data reveal tendencies of different residence times. Obviously groundwater collected in well 2 has a very large component of old water. The tritium activity of this sample (0.5 TU) is in the range of the detection limit. Nevertheless, the time of recharge, with some caution, must have been more than 10,000 years ago.

355 Furthermore groundwater collected in well 30 has also a low radiocarbon concentration (26 pmC) and consequently a longer residence time.

Several samples collected from wells with similar depths and arranged along a plausible north-south evolutionary flowpath (3-14-15-16-17; see Fig. 2) were modeled geochemically using the program NETPATH. The radiocarbon activity decreases from 109.0 to 45.9 pmC and $\delta^{13}\text{C}$ increases from -11.91 to -8.38 ‰ along this transect. Well 3 is most appropriate as initial water because of high radiocarbon activities but low $\delta^{13}\text{C}$ ratios. After Plummer and Sprinkle (2001) the carbon-isotope mass balance was solved assuming rain water reacting with calcite, dolomite, gypsum and soil CO_2 ($\delta^{13}\text{C} = -23$ ‰) to produce the water in the initial well 3 that probably was affected by post-bomb ^{14}C or irrigation return flow. Infiltration processes are subsequently described more thoroughly with the help of trace gases. The initial activity of ^{14}C was modelled with the help of a theoretical rain water whose composition was taken from Mahlkecht et al. (2004) referring to measurements in the Sierra de Guanajuato. Ca, Mg, S and total inorganic carbon (TIC) served as constraints and calcite, dolomite, gypsum and soil CO_2 as phases. To reproduce the $\delta^{13}\text{C}$ of -11.91 an exchange of 9 mmol CO_2/l was necessary which would simulate open system conditions. The corresponding ^{14}C activity in this case is 81 pmC. This value was used in further flowpath calculations as initial A_0 .

360

365

370

In the subsequent calculations also an exchange of Na and Ca / Na was inserted as a constraint to account for increasing Na but decreasing Ca values along the flow path. Sodium might originate from exchange on clay minerals. According to model calculations, groundwater needs 1,600 years for passing through the selected flowpath of 18 km (11.3 m/yr). It becomes apparent that solution of

375 carbonates is not the primary alteration process for ^{13}C and ^{14}C content. If soil CO_2 was not considered in the model, the $\delta^{13}\text{C}$ ratio would be more enriched and not match the observed values. The measured $\delta^{13}\text{C}$ can be computed, if CO_2 gas is considered with a pre-defined amount undergoing isotope exchange,. Dunkle et al. (1993) assume that open-system isotopic evolution generally may be limited to the unsaturated zone. However, as illustrated in our study results, CFCs
 380 enrichment took place due to irrigation return flow; and, therefore, the open system conditions along the flow path were assumed

Table 1: Results of MRTs and time lag calculations for CFC-12. Activities and MRTs for tritium are also included

Sample	CFC-12							Tritium	
	Conc.	Equ. air conc.	^a MRT	^b Time lag	^c Mean time lag	Corr. MRT	^d Dev.	Activity	MRT
	[pmol/l]	[pptv]	[years]	[years]	[years]	[years]	[pptv]	[TU]	[years]
1								3.5	50
2								0.5	>300
3	1.60	525	7	16	^e n.c.	n.c.	520	0.2	>300
4	0.03	10	>300	44	^f (230)	n.c.	6	2.9	73
5	0.55	180	70	20	51	19	170	0.7	>300
6								0.4	>300
7	0.90	298	35	20	28	7	283	0.9	>300
8	1.00	328	29	24	29	0	323	0.8	>300
9	1.00	328	29	14	17	12	302	1.0	300
10	0.58	190	65	30	62	3	186	0.6	>300
11	1.70	559	0	cont	cont	cont		0.9	>300
12	0.41	134	100	12	45	55	134	0.0	>300
13	0.48	157	83	15	46	37	143	0.6	>300
14	1.50	493	10	cont	cont	cont		1.3	220
15	0.80	262	42	24	37	5	252	0.9	>300
16	0.35	115	120	34	117	3	114	0.1	>300
17	1.40	459	14	29	n.c.	n.c.	459	0.0	>300
18	0.55	181	70	16	40	30	147	1.4	200
19	0.51	167	77	24	63	14	160	0.6	>300
20	0.84	276	39	41	n.c.	n.c.	275	0.2	>300
21	0.17	56	266	20	191	75	56	0.0	>300
22	1.00	328	29	33	n.c.	n.c.	325	2.0	128
23	1.20	393	21	13	n.c.	n.c.	343	1.6	170
24	0.27	88	161	27	138	23	87	0.1	>300
25	0.41	134	270	44	-	-	133	0.1	>300
26								0.0	>300
27	0.43	141	95	34	94	1	140	0.1	>300

28	0.71	235	50	36	n.c.	n.c.	235	0.0	>300
29	0.07	23	>300	32	(250)	n.c.	23	0.0	>300
30	0.11	36	>300	29	(250)	n.c.	35	0.1	>300

^a indicates mean residence time following the exponential flow model

385 ^b is the time lag calculated applying the analytical method of Cook and Solomon (1995)

^c is the correction of exponential model MRTs in years

^d horizontal deviation of the samples from EM model curve

^e not calculable. Because of high air concentrations and/ or large time lags corrected MRTs are out of range

^f values are in brackets because of very low concentrations

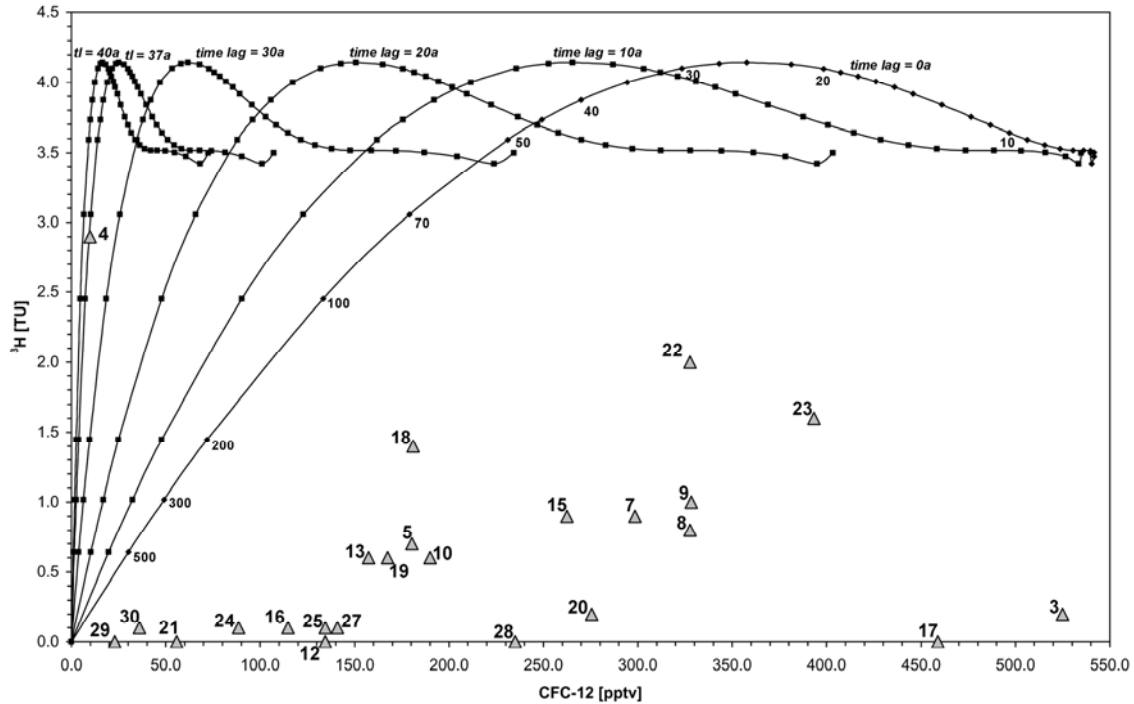
390

5.2 Recharge and Infiltration Processes

The discrepancy between ³H and CFC-12 is illustrated in Fig. 9 which shows the curves of the exponential model for different time lags. Unaffected samples should plot along the model lines.

Because increased CFC ratios are supposed to be caused by the impact of irrigation return flow, the
 395 deviation from the curve - i.e. the horizontal distance from the EM model lines in Fig. 9 - was taken as a qualitative estimation of the magnitude of return flow. To determine this deviation, the time lag was calculated for each well according to Cook and Solomon (1995) and the corresponding exponential model curve constructed. There are only 4 samples showing little (wells 21, 29, 30) or no impact (well 4) of irrigation return flow because the deviations from the corresponding model
 400 lines are within or close to the error intervals. The remaining samples present deviations of up to 520 pptv. The results of time lag calculations for CFC-12 are given in table 1.

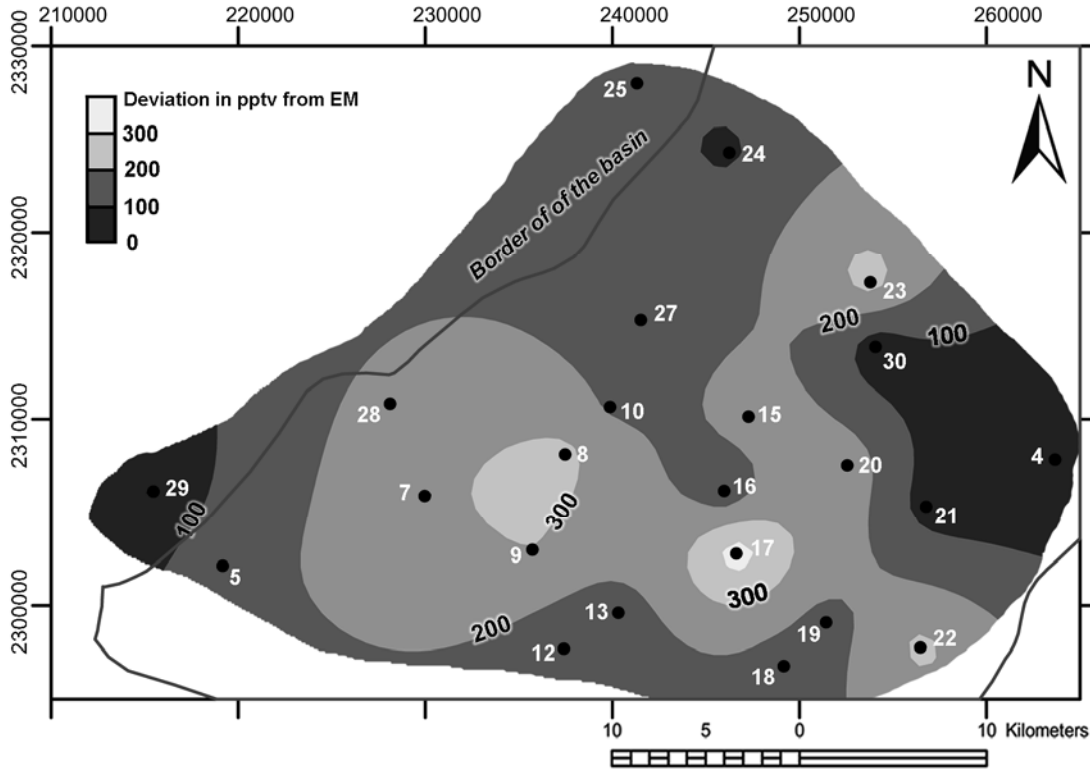
In regions without or with negligible irrigation return flow the construction of exponential model curves (see Fig. 9) helps to find and validate calculated time lags. This can be demonstrated with well 4. For this sample point a time lag of 44 years was calculated. The graphical solution yields 37
 405 years and confirms the calculation. Taking into account analytical errors, a minimum time lag of 26 years would be the result.



410 **Fig. 9 Hypothetical concentrations of tritium activities for the exponential model (EM) plotted versus the CFC-12-EM-concentrations. The different curves represent different time lags for CFC-12. The numbers along the first curve indicate the different mean residence times.**

As mentioned above, the deviation from the exponential model line might be considered as a magnitude of irrigation return flow impact as demonstrated graphically in Fig. 10. The samples which are probably affected by anthropogenic CFC contamination like pollution through waste dumps (wells 11 and 14) are not included. Another type of contamination might occur through the operation of wells and resulting water table fluctuations which constrain the introduction of fresh air (Li and Jiao, 2005). In this case, primarily the CFC ratios would increase because of very low concentrations and therefore rapid dissolution of gases. Influences of so-called excess air is another process but its content is less than 6 cm³/l (Wilson and McNeill 1997) and effects are supposed to be rather minor in comparison to the afore mentioned.

415



420

Fig. 10 Distribution of irrigation return flow impact. The numbers indicate the deviation of the equivalent air concentration of the samples from the expected EM concentrations in pptv of CFC-12. Lighter-coloured areas indicate a higher grade of return flow. Dark grey areas present a lower effect of irrigation return flow (<100 pptv CFC-12).

425 In comparison, radiocarbon activities might be affected less because the CO₂ partial pressure in groundwater is supposed to be higher than the atmospheric one and during the short time of extraction and sampling only degassing may take place leading at most to minor fractionation processes (Clark and Fritz 1997). CFC-12 and ¹⁴C are correlated significantly after Spearman's rho and Kendall's tau b on the 0.01 level. This correlation is caused by both natural recharge and

430 irrigation return flow because these processes not only modify CFC-12 concentrations but also change radiocarbon activities due to mainly exchange with modern soil CO₂ in the agriculturally used areas. An exception is – apart from the already excluded wells 3, 11 and 14 – well 17 presenting high CFC-12 ratios in comparison to relatively low ¹⁴C activities. The CFC enrichment could be related to water table fluctuation or to errors in the sampling procedure (Fig. 11). A further

435 validation of these processes would be possible with the help of noble gases (e.g. Wilson and McNeill 1997).

The agricultural influence is also reflected in nitrate concentrations. The nitrate in groundwater reaches values of up to 60 mg/l, although two cases show exceptionally high contents (154 mg/l in well 1 and 129 mg/l in well 14). There is a significant positive correlation between nitrate and ¹⁴C
 440 on the 0.01 level (nonparametric test of Spearman's rho and Kendall's tau b; Fig. 12). The nitrate values increase with higher radiocarbon activities. The corresponding wells with higher concentrations are situated primarily in the centre of the basin. There the tritium activities are low and therefore it is supposed that nitrate is transported mainly by infiltrating irrigation waters. Assuming that one third (650 km²) of the study area is irrigated by approximately 350 · 10⁶ m³/yr
 445 (CEAG, 2003) 500 mm of irrigation waters are introduced additionally to the rainfall. Thus the annual irrigation amount almost equals the annual precipitation.

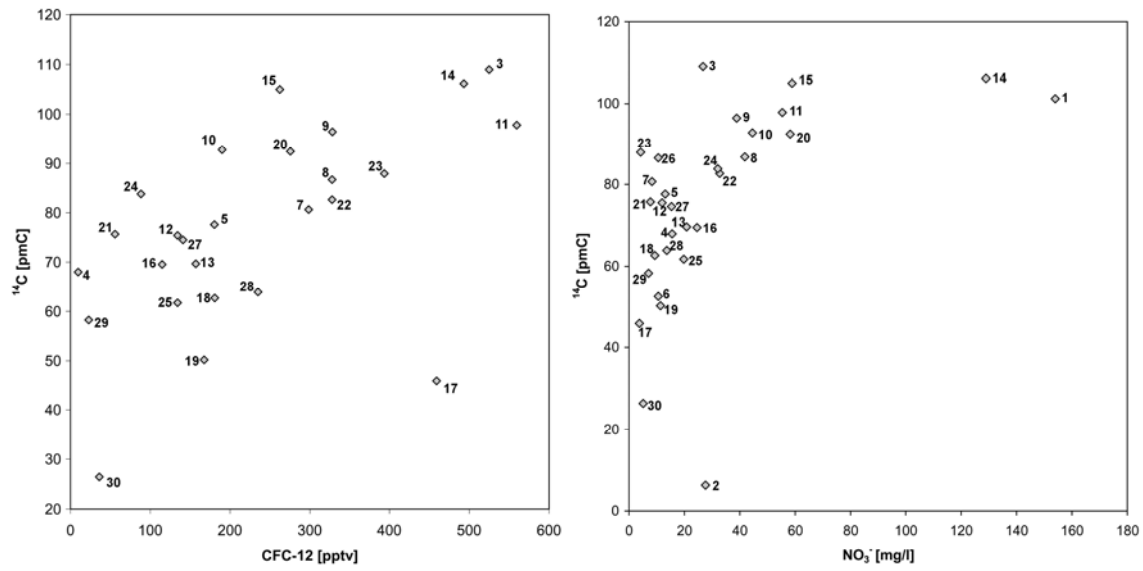


Fig. 11: Correlation of ¹⁴C and CFC-12 450 Fig 12 Radiocarbon activities versus nitrate confirm the impact of irrigation return flow. concentrations show a positive correlation.

6 Summary and Conclusion

455 Despite the strongly modified groundwater regime due to heavy exploitation of water resources
from the Silao-Romita aquifer system, it was possible to describe the main recharge processes and
to localise the principal zones of recharge. The recharge consists of a natural and an anthropogenic
component. The anthropogenic component has been recognized basically as irrigation return flow.
Natural vertical recharge is small in the centre of the basin which is indicated by low tritium
460 activities.

By contrast, the irrigation-induced recharge identified by increased CFC ratios is localised in areas
mainly inside the basin. Contaminants are transported to the saturated zone primarily by these
infiltrating irrigation excesses, as evidenced by nitrate distribution.

Radiocarbon activities in groundwater also showed the effect of return flow in the irrigation areas.

465 The geochemical modelling in uncontaminated groundwater showed that CO₂ exchange in recharge
areas and carbonate dissolution are the two main processes that have to be taken into account for
corrections of the ¹⁴C data. The ¹⁴C activity values are low in two cases and indicate larger
residence times of several thousand years. A more reliable estimation of mean residence times is
obtained by the interpretation of tritium activities. It yields mean residence times of 70 to more than
470 300 years applying the exponential flow model. Its conservative character gives furthermore an
insight into the natural recharge distribution but low activities impede a more precise interpretation.

The trace gas contents are enriched in most wells and do not serve for groundwater dating.

However, comparing CFCs with tritium, the degree of enrichment becomes apparent which
indicates the dimension and distribution of irrigation return flow. The applied graphic method is
475 applicable to verify the conventional time lag calculation through thick unsaturated zones if return
flow can be excluded.

7 Acknowledgements

The authors acknowledge the grant received from Consejo de Ciencias y Tecnología del Estado de Guanajuato (contract no. 04-12-A-044). Complementary funds have been contributed by the
480 Tecnológico de Monterrey, Campus Monterrey. A. Horst thanks Deutscher Akademischer Auslandsdienst (DAAD) for financing the time of fieldwork in Mexico. The Comisión Estatal del Agua de Guanajuato (CEAG) kindly facilitated the access to former studies. Field assistance is acknowledged to L. Oliva-Soto and J. Chávez-Guevara. D. Hebert (TU BA Freiberg) facilitated the tritium analysis. H.J. Peter (TU BA Freiberg) performed chemical analyses. The Department of
485 Isotope Hydrology, Halle, Germany, of the Helmholtz Centre for Environmental Research made the ^{13}C -analysis of the rock samples.

8 References

- 490 Aranda-Gómez JJ, Aranda-Gómez JM, Nieto-Samaniego AF (1989) Consideraciones acerca de la evolución tectónica durante el Cenozoico de la Sierra de Guanajuato y la parte meridional de la Mesa Central (Considerations of the tectonic evolution during the Cenozoic of the Mountains of Guanajuato and the southern part of the Central Highland) . *Rev Mex Cienc Geol* 8(1):33-46.
- Beyerle U, Aeschbach-Hertig W, Hofer M, Imboden DM, Baur H, Kipfer R (1999): Infiltration of river water to a shallow aquifer investigated with $^3\text{H}/^3\text{He}$, noble gases and CFCs. *J Hydrol* 220: 169-185
- 495 Böhlke JK (2004) TRACERMODEL1. Excel workbook for calculation and presentation of environmental tracer data for simple groundwater mixtures. In: IAEA Guidbook on the Use of Chlorofluorocarbons in Hydrology. International Atomic Energy Agency, Vienna, (in press). Available via USGS website http://water.usgs.gov/lab/software/tracer_model/
- 500 Bu X, Warner MJ (1995) Solubility of chlorofluorocarbon 113 in water and seawater. *Deep-Sea Research* 42(7):1151–1161.
- Burbach G, Frolich C, Pennington W, Matumoto T (1984) Seismicity and tectonics of the subducted Cocos plate. *J Geophys Res* 89:7719-7735.
- 505 CEAG - Comisión Estatal del Agua de Guanajuato (2003) Cuantificación del volumen de extracción a partir del Análisis de Imágenes de Satélite y Verificación de Campo en el Acuífero Silao- Romita, Gto (Quantification of the extracted volume using satellite image análisis and verification in field in the aquifer of Silao-Romita, Gto) performed by Gondwana Exploraciones , Guanajuato, Mexico. Report
- 510 CEASG - Comisión Estatal del Agua y Saneamiento de Guanajuato (1998) Estudio Hidrogeológico y Modelo Matemático del Acuífero del Valle de Silao Romita, Gto. (Hydrogeological study and mathematical model of the aquifer of the valley of Silao-Romita, Gto). Contrat no. CEAS-APA-GTO-97-025, performed by Lesser y Asociados SA de CV, Mexico. Report

- CEASG (1999) Estudio isotópico para la caracterización del agua subterránea en la zona de La Muralla, Guanajuato (Isotope study for the characterization of the groundwater in the zone of La Muralla, Guanajuato). Contract no. CEASXXVI- OD-UNAM-99-088, performed by Instituto de Geofísica, Universidad Nacional Autónoma de México, Mexico, 74 p. Report
- 515 CEASG (2001) Sinopsis – Estudios hidrogeológicos y modelos matemáticos de los acuíferos del estado de Guanajuato (Hydrogeologic studies and mathematic models of the aquifers of the Guanajuato State). Compact disc. Comisión Estatal del Agua y Saneamiento de Guanajuato, Guanajuato, Mexico.
- Clark IA, Fritz P (1997) Environmental Isotopes in Hydrogeology, Lewis Publishers, New York
- 520 Cook PG, Solomon DK (1995) Transport of atmospheric trace gases to the water table: Implications for groundwater dating with chlorofluorocarbons and Krypton 85, *Wat Resour Res* 31(2):263-270.
- COREMI/ CONCyTEQ/ CENICA, Dirección Técnica, Subdirección De Apoyo Técnico, Gerencia De Estudios Especiales, Subgerencia de Geohidrología y Geotecnia (2004): Potencial geohidrológico del Graben De Leon (Hydrogeological potential of the León Graben), Pachuca, HGO. Report
- 525 Dunkle SA, Plumier LN, Busenberg E, Phillips PJ, Denver JM, Hamilton PA, Michel RL, Coplen TB (1993): Chlorofluorocarbons (CCl₃F and CCl₂F₂) as dating tools and hydrologic tracers in shallow groundwater of the Delmarva Peninsula, Atlantic Coastal Plain, United States. *Wat Resour Res* 29 (12): 3837-3860
- Engesgaard P, Højberg AL, Hinsby K, Jensen KH, Laier T, Larsen F, Busenberg E, Plummer LN (2004) Transport and time lag of chlorofluorocarbon gases in the unsaturated zone, Rabis Creek, Denmark. *Vadose Zone J* 3:1249-1261.
- 530 Foster S, Garduño H, Kemper K (2004) The ‘COTAS’ – Progress with stakeholder participation in groundwater management in Guanajuato-Mexico. Case Profile Collection No. 10, GW Mate, World Bank. 10p.
- Happell, J.D.; S. Opsahl, Z. Top and J.P.Chanton (2006): Apparent CFC and ³H/³He differences in water from Floridan Aquifer springs. *J. Hydrol.* 319: 410-426
- 535 Horst A, Mählknecht J and Merkel B J (2007) Estimating groundwater mixing and origin in an overexploited aquifer in Guanajuato, Mexico, using stable isotopes (strontium-87, carbon-13, deuterium and oxygen-18), *Isot Environ Health S*, 43:4, 323 – 338
- Li, H. and J.J. Jiao (2005): One-dimensional airflow in unsaturated zone induced by periodic water table fluctuation, *Water Resour. Res* 41, doi:10.1029/2004WR003916
- 540 Lindsey BD, Phillips SW, Donnelly CA, Speiran GK, Plummer LN, Böhlke JK, Focazio MJ, Burton WC, Busenberg E (2003) Residence times and nitrate transport in ground water discharging to streams in Chesapeake Watershed, WRI Report 03-4035, US Geological Service, New Cumberland, Pennsylvania, USA, 215 p. available via USGS website: <http://pa.water.usgs.gov/reports/wrir03-4035.pdf>
- Mählknecht J, Schneider JF, Merkel BJ, Navarro de León I, Bernasconi SM (2004) Groundwater recharge in a sedimentary basin in semi-arid Mexico. *Hydrogeol J* 12 (5):511-530.
- 545 Matter JM, Waber HN, Loew S, Matter A (2005) Recharge areas and geochemical evolution of groundwater in an alluvial aquifer system in the Sultanate of Oman. *Hydrogeol J* 14:203-224
- Nieto-Samaniego AF, Macías-Romo C, Alaniz-Alvarez SA (1996) Nuevas edades isotópicas de la cubierta volcánica cenozoica de la parte meridional de la Mesa Central (New isotopic ages of the Cenozoic volcanic cover of the southern part of the Central Highland), México, *Rev Mex Cienc Geol* 13(1):117-122.
- 550 Oster H, Sonntag C, Munich KO (1996): Groundwater age dating with chlorofluorocarbons. *Wat Resour. Res* 32 (10): 2989-3001
- SAPAL - Sistema de Agua Potable y Alcantarillado de León (2001) Estudio Isotópico e Hidrogeoquímico de la Zona de León-Río Turbio (Isotopic and hydrochemical study of the León-River Turbio Zone), performed by Instituto de Geofísica, Universidad Nacional Autónoma de México, Mexico, Report

- 555 Pardo M, Suárez G (1993) Steep subduction geometry of the Rivera plate beneath the Jalisco block in western Mexico, *Geoph Res Lett* 20:2391-2394.
- Plummer LN, Busenberg E (2000) Chlorofluorocarbons. In: Cook P, Herczeg AL: *Environmental Tracers in Subsurface Hydrology*, Kluwer Academic Publishers, Boston,
- 560 Plummer LN, Prestemon EC, Parkhurst DL (1994) An interactive code (NETPATH) for modeling net geochemical reactions along a flow path, version 2.0. USGS Wat Res Invest Rep 94-4169.
- Plummer LN, Sprinkle CL (2001): Radiocarbon dating of dissolved inorganic carbon in groundwater from confined parts of the Upper Floridan aquifer, Florida, USA. *Hydrogeol J* 9:127-150
- Warner MJ, Weiss RF (1985) Solubilities of chlorofluorocarbons 11 and 12 in water and seawater. *Deep-Sea Res* 32:1485-1497.
- 565 Weiss RF, Price BA (1980) Nitrous oxide solubility in water and seawater. *Mar Chem* 8:347-359.
- Weissmann, G. S., Y. Zhang, E. M. LaBolle, and G. E. Fogg, (2002) Dispersion of groundwater age in an alluvial aquifer system. *Water Resour. Res.*, 38(10), 1198, doi:10.1029/2001WR000907
- Wilson GB and McNeill GW (1997): Noble gas recharge temperatures and the excess air component. *App Geochem* 12: 747-762
- 570 Zuber A (1986) Mathematical models for the interpretation of environmental radioisotopes in groundwater systems In: Fritz P. and J.Ch. Fontes: *Handbook of environmental isotope geochemistry, Volume 2; The Terrestrial Environment*, B; Elsevier, Amsterdam a.o.;
- Zuber A.; S.M. Weise, J. Motyka, K. Osenbrück and K. Róžański (2004): Age and flow pattern of groundwater in a Jurassic limestone aquifer and related Tertiary sands derived from combined isotope, noble gas and chemical data. *J. Hydrol* 286: 87-112
- 575

Appendix

Table 1 Results of field parameters and analyses of some major elements (^a indicates that no measurement was done; ^b Bold italic water levels are from 2004 because of inaccessibility in 2005 (unpublished data of the local water agency CEAG); ^c values are not known; ^d values in brackets are an estimation

Sample	Location	Type	water level (m)	Tot. depth (m)	Temp. (°C)	pH	EC (µS/cm)	TIC [mg/l]	Na ⁺ [mg/l]	Ca ²⁺ [mg/l]	Mg ²⁺ [mg/l]	NO ₃ ⁻ [mg/l]	SO ₄ ²⁻ [mg/l]
1	Sangre de Cristo	spring	0	0	16.3	7.8	^a --	41.2	61.7	94.6	89.5	154.0	307.0
2	Hotel Comanjilla	therm.spring	0	0	96.3	8.7	--	59.3	150.0	56.1	40.7	27.6	47.6
3	Rancho Bustamante	well	^b 57	300	22.8	7.1	911	42.1	80.4	32.1	36.0	26.7	46.6
4	Zangarro	well	135	300	27.2	7.4	636	52	82.7	20.8	9.0	15.6	34.2
5	San Ramon	well	69	180	24.4	7.4	623	47.5	30.8	22.4	7.2	13.1	24.0
6	Ojos De Rana	well	69	135	29.6	7.4	526	36.7	62.0	20.8	9.0	10.6	35.2
7	Prodencia	well	69	150	24.0	7.3	2860	55.1	413.0	176.0	29.6	8.3	689.0
8	Fracción El Sillero	well	78	150	27.3	7.4	610	67.6	47.9	67.3	23.6	41.8	37.5
9	San Clemente	well	53	100	23.8	7.3	1006	52.3	107.0	25.7	10.0	38.9	113.0
10	Granja Lupita	well	96	150	26.2	7.4	647	69.3	53.9	70.5	21.8	44.6	26.8
11	R. Sagrado Cor. D.Jes.	well	101	350	23.0	7.4	1271	90	79.1	144.0	39.3	55.4	330.0
12	Vista Hermosa	well	46	70	25.5	7.3	600	67.3	60.5	54.5	17.6	11.9	35.4
13	Ejido Tejamanil	well	54	100	24.0	7.4	594	65	42.9	64.1	19.8	20.8	36.1
14	L-1036	well	69	100	22.7	7.2	1261	101	45.2	91.4	63.4	129.0	80.1
15	El Renadito	well	80	200	24.0	7.3	867	84.6	34.3	103.0	37.7	58.9	66.4
16	Las Trojas	well	106	300	27.6	7.3	617	63.1	50.0	52.9	22.2	24.6	42.1
17	Trejo Ej. Benavente	well	93	117	25.0	7.6	536	54.9	61.4	28.9	15.6	3.8	35.6
18	Ro. Gpe Paso Blanco	well	56	150	29.0	7.6	1334	75.1	185.0	32.1	12.7	9.4	285.0
19	Ro. Granja los Cedros	well	78	200	27.8	7.3	944	62.6	107.0	65.7	22.9	11.4	147.0
20	La Purisma d. I.Torres	well	125	300	22.8	7.2	765	83.7	54.2	94.6	12.7	58.2	37.5
21	San Vicente	well	68	250	27.7	7.7	453	39.2	38.5	36.9	11.3	7.7	19.5
22	Lo de Juarez	well	105	160	26.3	7.4	587	28.5	12.9	67.3	8.3	32.8	51.2
23	Los Rodriguez	well	48	300	24.0	7.3	623	69.5	41.6	57.7	30.6	4.2	52.5
24	Rancho San Agustin	well	86	500	27.3	7.4	664	67.4	11.8	57.7	34.2	32.1	38.1
25	San. José d.l. Romeros	well	150	^c ?	28.3	7.3	630	59.4	66.4	40.1	15.1	19.8	11.2
26	Ej. Playas de Sotelo	well	98	180	28.4	7.6	546	71.4	62.7	49.7	5.8	10.6	29.4
27	Ej. Guadalupe Ramales	well	107	?	27.1	7.6	570	63.5	45.1	54.5	18.7	15.3	27.4
28	Rancho la Joga	well	113	190	29.0	7.7	2510	13.8	148.0	501.0	10.6	13.6	1832.0
29	Balneario Tres Villas	well	^d (100)	170	34.7	7.4	656	42.8	88.7	38.5	5.5	7.0	133.0
30	Agua P. San Ignacio	well	93	350	30.2	7.7	816	70.1	71.6	40.1	6.4	5.2	144.0

Table 2: Results of tritium and carbon isotope analysis. (^a indicates mean residence time following the exponential flow model; ^b uncorrected data; ^c is the correction factor for carbonate dissolution; ^d rec. indicates recent conditions)

Sample	Tritium			Carbon isotopes					
	Conc. (TU)	St.dev. (2-σ)	^a MRT (years)	¹⁴ C pmC	δ ¹³ C ‰ VPDB	MRT ^b uncorr. years	¹³ C correction model		
							¹³ C _{rech}	^c q	years
1	3.5	0.6	50	101.23	-10.46	302	-11.4	0.9	^d rec.
2	0.5	0.4	>300	6.32	-9.28	23232	-18.2	0.3	14400
3	0.2	0.4	>300	108.95	-11.91	799	-13.2	0.8	rec.
4	2.9	0.5	73	67.99	-7.88	4697	-13.0	0.4	rec.
5	0.7	0.4	>300	77.6	-7.51	2500	-12.7	0.4	rec.
6	0.4	0.4	>300	52.49	-8.10	5732	-13.2	0.4	rec.
7	0.9	0.4	>300	80.67	-10.38	2179	-12.7	0.7	rec.
8	0.8	0.4	>300	86.76	-9.35	1577	-12.9	0.6	rec.
9	1.0	0.4	300	96.42	-8.80	1809	-12.8	0.5	rec.
10	0.6	0.4	>300	92.78	-9.00	1023	-12.8	0.5	rec.
11	0.9	0.4	>300	97.77	-10.13	590	-12.6	0.7	rec.
12	0.0	0.3	>300	75.42	-8.55	2735	-12.9	0.5	rec.
13	0.6	0.4	>300	69.66	-9.56	3392	-12.6	0.6	rec.
14	1.3	0.4	220	106.14	-9.71	1015	-12.9	0.6	rec.
15	0.9	0.4	>300	104.95	-9.45	1108	-12.7	0.6	rec.
16	0.1	0.4	>300	69.53	-8.96	3408	-13.2	0.5	rec.
17	0.0	0.3	>300	45.88	-8.38	6845	-12.5	0.5	800
18	1.4	0.4	200	62.69	-9.74	5368	-12.8	0.6	400
19	0.6	0.4	>300	50.2	-9.45	6101	-13.1	0.6	1500
20	0.2	0.4	>300	92.46	-9.42	1051	-13.0	0.6	rec.
21	0.0	0.3	>300	75.7	-7.60	2705	-12.7	0.4	rec.
22	2.0	0.5	128	82.66	-8.61	3082	-12.9	0.5	rec.
23	1.6	0.5	170	87.96	-9.61	2568	-12.7	0.6	rec.
24	0.1	0.4	>300	83.84	-9.13	1860	-13.0	0.5	rec.
25	0.1	0.4	>300	61.72	-6.87	4393	-13.2	0.3	rec.
26	0.0	0.3	>300	86.57	-8.47	1596	-12.9	0.5	rec.
27	0.1	0.3	>300	74.55	-8.63	2831	-12.8	0.5	rec.
28	0.0	0.3	>300	63.92	-10.62	4103	-12.8	0.7	rec.
29	0.0	0.3	>300	58.24	-8.05	4872	-13.6	0.4	rec.
30	0.1	0.4	>300	26.41	-7.18	11410	-12.9	0.3	1700

Table 3: Results of trace gas analyses. (^a describes the equivalent air concentration determined with the corresponding input functions; ^b indicates the mean residence time following the exponential flow model; ^c describes the effect of the unsaturated zone thickness on the residence time (piston flow); ^d is the correction of exponential model MRTs in years; ^e dev describes the deviation of trace gas concentration from the supposed EM values in pptv.; ^f values in brackets because of very low concentrations

Sample	CFC-11				CFC-113				CFC-12							
	Concentration		^a AAC	^b MRT	Concentration		AAC	MRT	Concentration		AAC	MRT	^c Time lag	^d Mean t. lag	Corr. MRT	^e Deviation
	(pmol/l)	1- σ	(pptv)	(years)	(pmol/l)	1- σ	(pptv)	(years)	(pmol/l)	1- σ	(pptv)	(years)	(years)	(years)	(years)	(pptv)
3	2.30	0.30	204	19.0	0.23	0.05	69	11.0	1.60	0.10	525	7	16	-	-	520
4	0.06	0.05	5	> 300	<0.01	-	3	>300	0.03	0.05	10	>300	44	^f (230)	-	6
5	0.60	0.10	53	127.0	0.08	0.05	24	67.0	0.55	0.05	180	70	20	51	19	170
7	1.20	0.20	108	56.0	0.14	0.05	42	31.8	0.90	0.10	298	35	20	28	7	283
8	1.20	0.20	107	56.0	0.15	0.05	45	28.7	1.00	0.10	328	29	24	29	0	323
9	1.20	0.20	107	56.0	0.12	0.05	36	39.7	1.00	0.10	328	29	14	17	12	302
10	0.90	0.10	80	82.0	0.08	0.05	24	67.0	0.58	0.05	190	65	30	62	3	186
11	1.90	0.20	169	27.7	0.15	0.05	45	28.7	1.70	0.10	559	0	cont	cont	cont	
12	0.53	0.10	47	148.0	0.07	0.05	21	78.7	0.41	0.05	134	100	12	45	55	134
13	0.49	0.05	44	164.0	0.07	0.05	21	78.5	0.48	0.05	157	83	15	46	37	143
14	2.20	0.30	196	20.6	0.11	0.05	33	44.7	1.50	0.10	493	10	cont	cont	cont	
15	1.00	0.10	89	71.0	0.11	0.05	33	44.7	0.80	0.10	262	42	24	37	5	252
16	0.54	0.10	48	145.0	0.05	0.05	15	115.0	0.35	0.05	115	120	34	117	3	114
17	1.70	0.20	151	33.6	0.21	0.05	63	14.6	1.40	0.10	459	14	29	n.c.	-	459
18	0.61	0.10	54	127.5	0.06	0.05	18	94.0	0.55	0.05	181	70	16	40	30	147
19	0.63	0.10	56	122.4	0.07	0.05	21	78.5	0.51	0.05	167	77	24	63	14	160
20	1.20	0.20	107	56.0	0.10	0.05	30	50.7	0.84	0.10	276	39	41	-	-	275
21	0.18	0.05	16	> 300	0.03	0.05	9	200.0	0.17	0.05	56	266	20	191	75	56
22	1.50	0.20	133	40.9	0.15	0.05	45	28.7	1.00	0.10	328	29	33	-	-	325
23	1.80	0.20	160	30.2	0.19	0.05	57	18.9	1.20	0.10	393	21	13	-	-	343
24	12.00	3.00	1065	cont.	0.04	0.05	12	148.0	0.27	0.05	88	161	27	138	23	87
25	0.43	0.05	38	>300	0.06	0.05	18	200.0	0.41	0.05	134	270	44	-	-	133
27	0.70	0.10	62	109.0	0.07	0.05	21	78.5	0.43	0.05	141	95	34	94	1	140
28	1.10	0.20	99	62.0	0.11	0.05	33	44.7	0.71	0.10	235	50	36	-	-	235
29	0.12	0.05	11	>300	0.02	0.05	6	>300	0.07	0.05	23	>300	32	(250)	-	23
30	0.10	0.05	9	>300	0.02	0.05	6	>300	0.11	0.05	36	>300	29	(250)	-	35